CHEMISTRY OF MATERIALS

Article

pubs.acs.org/cm

Stability of DNA Origami Nanostructure under Diverse Chemical Environments

Hyojeong Kim, Sumedh P. Surwade, Anna Powell, Christina O'Donnell, and Haitao Liu*

Department of Chemistry, University of Pittsburgh, 219 Parkman Avenue, Pittsburgh, Pennsylvania 15260, United States

Supporting Information

ABSTRACT: We report the effect of chemical and physical treatments on the structural stability of DNA origami nanostructures. Our result shows that DNA nanostructure maintains its shape under harsh processing conditions, including thermal annealing up to 200 °C for 10 min, immersing in a wide range of organic solvents for up to 24 h, brief exposure to alkaline aqueous solutions, and 5 min exposure to UV/O_3. Our result suggests that the application window of DNA nanostructure is significantly wider than previously believed.

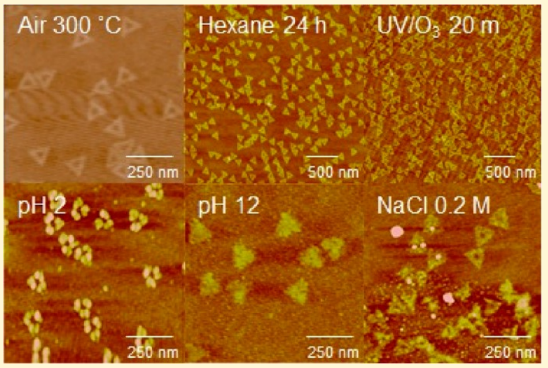

INTRODUCTION

The past decade has witnessed an explosive growth in the design and synthesis of DNA nanostructures. Through careful design of sequences, almost any desired 2D and 3D shapes can be constructed with nanometer scale precision and accuracy. Examples of such structures include individual 2D and 3D objects,[1−6] 1D nanowires and nanotubes,[7,8] 2D lattices,[9] and 3D crystals.[10]

Many of the applications of DNA nanostructures take advantage of their precise and highly configurable geometries. DNA nanostructures have been used as templates to pattern and direct the assembly of various biomolecular, organic, and inorganic materials, including metal nanoparticles,[8,11−19] proteins,[11,12,20,21] carbon nanotubes,[22,23] and quantum dots.[24] In addition, efforts have also been made to use DNA as a template to directly or indirectly pattern graphene and inorganic oxide substrates.[25−29] For example, Becerril et al. used aligned DNA molecule as a shadow mask for angled metal vapor deposition.[25] A spatial resolution in the sub-10 nm range was demonstrated. Deng et al. reported the metal evaporation onto DNA nanostructures deposited on a mica substrate followed by lift-off to create metal replicas of DNA.[26] Recently we demonstrated the use of DNA nanostructures as a mask for the etching of SiO_2 and chemical vapor deposition of inorganic oxides; in both cases, both positive tone and negative tone pattern transfers were obtained through a careful control of the reaction conditions.[28,29]

Although significant progress has been made, using DNA nanostructures in the bottom-up fabrication still faces significant challenges. In particular, many bottom-up fabrications involve very harsh processing conditions such as high temperatures and corrosive chemicals. However, DNA is a soft, chemically labile material that has limited thermal and chemical stability. In fact, even widely used solution phase processes could pose a significant risk, since deposited DNA nanostructures could be easily lifted-off from the substrate.[13,17] Because of this reason, the success of a DNA-mediated bottom-up fabrication is often limited and constrained by the stability of DNA nanostructures themselves. Therefore, understanding their structural stability under various chemical and physical environments is critical to the advance of this field of research.

In aqueous solution, the kinetics and thermodynamics of DNA hybridization are well understood. Several groups have recently investigated the stability of DNA nanostructure in buffer solutions and physiological relevant environments.[30−32] Efforts have also been made to enhance the stability of DNA nanostructure in solution by cross-linking.[33,34]

In contrast to the rapid development in solution phase studies, little is known about the structural stability of DNA nanostructure that has been deposited onto a supporting substrate. Compared to the dissolved DNA nanostructures, the deposited ones are much more relevant to the bottom-up nanofabrication because it allow for the patterning of the substrate and convenient multistep processing of the DNA nanostructures. Despite its importance, to the best of our knowledge, there is no systematic study on the effect of physical and chemical processing conditions on the structural integrity of substrate-supported DNA nanostructures.

Herein we report a study on the structural stability of DNA nanostructures deposited on a silicon wafer under a wide range of chemical and physical processing conditions, including thermal annealing, washing with organic solvents and aqueous

Received: May 29, 2014
Revised: August 23, 2014
Published: August 25, 2014

   dx.doi.org/10.1021/cm5019663 | Chem. Mater. 2014, 26, 5265−5273

solvents, and UV/O_3 treatment. These processing conditions are chosen for their relevance to DNA-based bottom-up nanofabrications, including metallization of DNA nanostructures, DNA-mediated etching and chemical vapor deposition, and DNA-templated assembly of inorganic nanocrystals.

This study will only focus on the overall preservation of the *shape* of the DNA nanostructures because the geometry, rather than the chemical integrity of a DNA nanostructure, often plays the most important role for most DNA-based nanofabrications. Our result shows that DNA nanostructures, once deposited onto a silicon substrate, are surprisingly stable and survive very harsh treatments, including thermal annealing to 200 °C for 10 min, washing with various organic solvents and alkaline aqueous solutions, and 5 min of UV/O_3 treatment. The result suggests that the application window of DNA nanostructure is much wider than previously thought.

EXPERIMENTAL SECTION

Materials and Methods. Silicon wafers [110] and [100] with native oxide layers were purchased from University Wafers and SILTRONIC SINGAPORE Pte. Ltd., respectively. M13mp18 scaffold and synthetic staple DNA strands for fabricating the DNA nanostructures were from New England Biolabs and Integrated DNA Technologies, respectively. 2-Amino-2-(hydroxymethyl)-1,3-propanediol (Trizma base), ethylenediaminetetraacetic acid (EDTA), acetic acid (≥99.7%), magnesium acetate tetrahydrate, sulfuric acid, hydrogen peroxide solution (30% H_2O_2), sodium chloride (≥99.0%), ethanol, hexane (mixture of isomers, ≥98.5%), and toluene (≥99.5%) were purchased from Sigma-Aldrich (St. Louis, MO). Hydrochloric acid and sodium hydroxide were purchased from Fisher Scientific (Fair Lawn, NJ). All materials were used as received. Water (18.3 MΩ) was filtered by a water purification system (Barnstead EASYpure II or Barnstead MicroPure Standard, Thermo Scientific, Waltham, MA) and used throughout the entire experiment.

Preparation of Buffer Solution. Buffer solution was prepared by dissolving Trizma base, EDTA, acetic acid, and magnesium acetate tetrahydrate in deionized water where the concentrations of these reagents were 40 mM, 2 mM, 20 mM, and 150 mM, respectively. The buffer solution was further diluted with deionized water so that the final concentration of magnesium ion was 12.5 mM.

Synthesis of DNA Origami Nanostructures. M13mp18 scaffold DNA strand solution (8.6 μL, 1.6 nM) was thoroughly mixed with 15 μL of the desired set of 253 staple DNA strands solution (16 nM), 77 μL of deionized water, and 181 μL of the buffer solution. The mixed DNA solution was annealed and filtered following our previously published procedure.[28,29]

Deposition of DNA Origami Nanostructures onto Si Wafer. A Si wafer with a native oxide layer was cleaned by immersing it in a hot piranha solution (3/7 (v/v) hydrogen peroxide/sulfuric acid solution) for a minimum of 20 min. *Warning: Piranha solution is a strong oxidizing reagent and can detonate unexpectedly. Extra caution in handling is required.* The substrate was thoroughly washed with deionized water and dried with N_2 gas. DNA origami solution (2−3 μL) was pipetted onto a clean Si wafer and left undisturbed for 30 min inside a Petri dish with its lid covered by a moist kimwipe to minimize the evaporation of the buffer solution. The substrate was then dried by blowing N_2 gas followed by immersion in a 9/1 (v/v) ethanol/water solution for 3 s to remove salt impurities. The substrate was redried using N_2 gas.

Thermal Stability of DNA Origami Nanostructures in Air and Argon. The DNA origami nanostructures assembled on a Si wafer were placed inside a tube furnace (Lindberg/Blue M, Thermo Scientific, Waltham, MA) using a quartz support and temperature was elevated. The Si substrates with DNA nanostructures were heated at the desired temperature for 10 min and cooled down either in air or under the flow of argon (100 standard cubic centimeter per minute (SCCM)). For each desired temperature, AFM images of a minimum of two samples were taken before and after the heating. The average height of DNA nanostructures was obtained by measuring the heights of 12−24 DNA origami triangles. The change in height was calculated by comparing the average height of DNA nanostructures before and after the treatment.

Stability of DNA Nanostructures in Organic Solvents. The DNA origami nanostructures assembled on Si wafers were immersed in hexane, ethanol, or toluene solvents for 2, 4, or 24 h. The Si substrates with DNA nanostructure were dried with an N_2 stream.

Stability of DNA Nanostructures in Deionized Water. The DNA origami nanostructures assembled on Si wafers were immersed in deionized water for 10 s, 5 min, or 1 h. The Si substrates with DNA nanostructure were then dried with an N_2 stream.

Influence of Ionic Strength on the Stability of DNA Nanostructures. The DNA origami nanostructures deposited on a Si wafer were placed inside a sodium chloride solution of desired concentration (0.01−0.2 M) for 10 s followed by blow-drying with N_2 gas. Depending on surface cleanness, most of the samples were washed once or twice in the 9/1 (v/v) ethanol/water solution for 3 s to remove the salt impurities and then redried using N_2 gas to obtain clean AFM images.

Stability of DNA Origami Nanostructures as a Function of pH. The DNA origami nanostructures deposited on Si wafers were immersed in the solution of desired pH for 10 s and dried with N_2 gas. Acidic solutions were prepared by diluting hydrochloric acid with deionized water and pH values ranged from 2 to 4. Basic solutions were prepared by dissolving sodium hydroxide in deionized water and pH values ranged from 10 to 12.

Stability of DNA Origami Nanostructures Towards UV/O_3. The DNA origami nanostructures assembled on a Si wafer were subjected to UV/O_3 treatment for the desired time period at room temperature (PSD Series Digital UV Ozone Cleaner, Novascan Technologies, Inc., Ames, IA). Before UV/O_3 treatment, the cleaner was filled out with O_2 for 5 min. For each sample, two AFM images were taken at different locations before and after the treatment. The average height of DNA nanostructures was obtained by measuring the heights of 9−13 DNA origami triangles at each location. The change in height was calculated by comparing the average height of DNA nanostructure before and after the treatment.

Atomic Force Microscope (AFM) Measurements. Throughout the study, surface morphologies of the samples were monitored on a Veeco Dimension 3100 equipped with a Nanoscope IIIa controller by tapping mode in air. NSC15/AL_BS and NSC15/HARD/AL_BS AFM probes (325 kHz, 46 N/m and 40 N/m, respectively) were purchased from μmasch (Lady's Island, SC).

RESULTS AND DISCUSSION

We used a DNA equilateral triangle origami structure as a model in this study. The design of this DNA nanostructure minimizes bending within a structure and aggregation between structures; each edge of the DNA nanostructure consists of 9 parallel double stranded DNA and measures ∼140 nm in length.[4] The theoretical height of the DNA double helix is 2.0 nm although when measured by an AFM, the observed height could vary significantly due to the difference in sample-tip and substrate-tip interaction.[35,36] Our group has used this DNA nanostructure as the template for a number of bottom-up nanofabrication work, including etching and masking of SiO_2[28] and templated chemical vapor deposition of inorganic oxides.[29] For this study, the DNA nanostructures were deposited onto a silicon wafer with ∼1 nm thick layer of SiO_2. Previous study suggested that the interaction between DNA and SiO_2 is mediated by Mg^{2+} ions.[37,38]

Thermal Stability of DNA Origami Nanostructures. Many fabrication processes require treatment at high temperature. For example, chemical vapor deposition and atomic layer deposition often require heating sample up to several hundred

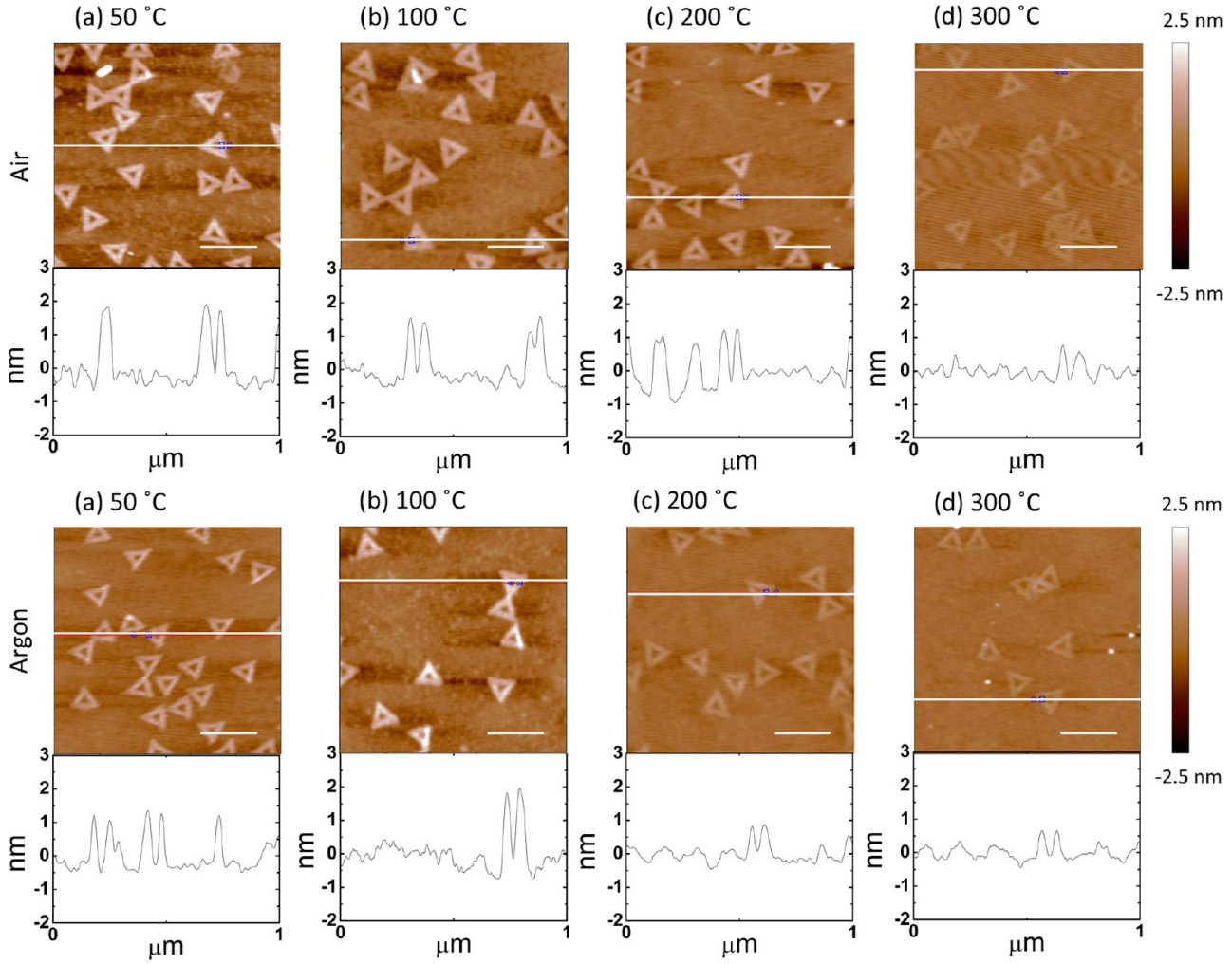

Figure 1. Thermal stability of DNA nanostructures in air and argon. AFM images of DNA origami triangles heated at (a) 50 °C, (b) 100 °C, (c) 200 °C, and (d) 300 °C for 10 min. White horizontal lines on the AFM images indicate where the cross sections were determined. Top: under air. Bottom: under argon. Scale bars: 250 nm.

degrees.[39−41] Therefore, it is important to understand the thermal stability of DNA nanostructures.

In solution, the structural stability of DNA nanostructures is limited by the melting (dehybridization) of double stranded DNA (ds-DNA). The melting temperature depends on the sequence of the ds-DNA and the composition of the buffer[42] but typically is in the range of 40−100 °C. However, when deposited onto a solid substrate and heated in a dry state, a DNA nanostructure could maintain its overall *shape* at a much higher temperature because the DNA strands are immobilized on the surface. In this case, the chemical stability of DNA itself becomes relevant. Aoi et al. used thermogravimetric analysis (TGA) to study the thermal decomposition of pure DNA film made by salmon DNA under a nitrogen atmosphere.[43] They observed that the decomposition started at 230 °C with two maxima of the decomposition rate at 233 and 300 °C; surprisingly, a residual weight of 53% was observed even after heating the sample to 500 °C. An interesting question here is whether the DNA nanostructure could keep its overall *shape* in the event of partial or even significant chemical decomposition.

To answer this question, we have evaluated the shape of DNA nanostructures under thermal stress. We deposited DNA origami triangles onto silicon wafers and heated the samples at various temperatures under both argon and air. The DNA structures were characterized by AFM before and after the heating to assess their topography. As shown in Figure 1, no apparent changes in the equilateral triangular *shape* were observed when the DNA nanostructures were heated up to 300 °C under both argon and air atmospheres. On heating beyond 200 °C, the DNA nanostructure likely decomposed, as indicated by a large decrease of the average height shown in Figure 2. It was found that the average height of the DNA nanostructures decreased by ∼50% after the heating at 250 °C

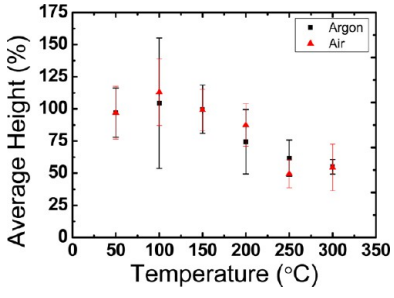

Figure 2. Effect of heating in air and argon on the relative height of the DNA nanostructures (n = 12−24). The data are normalized to the average height before the heating.

dx.doi.org/10.1021/cm5019663 | *Chem. Mater.* 2014, 26, 5265−5273

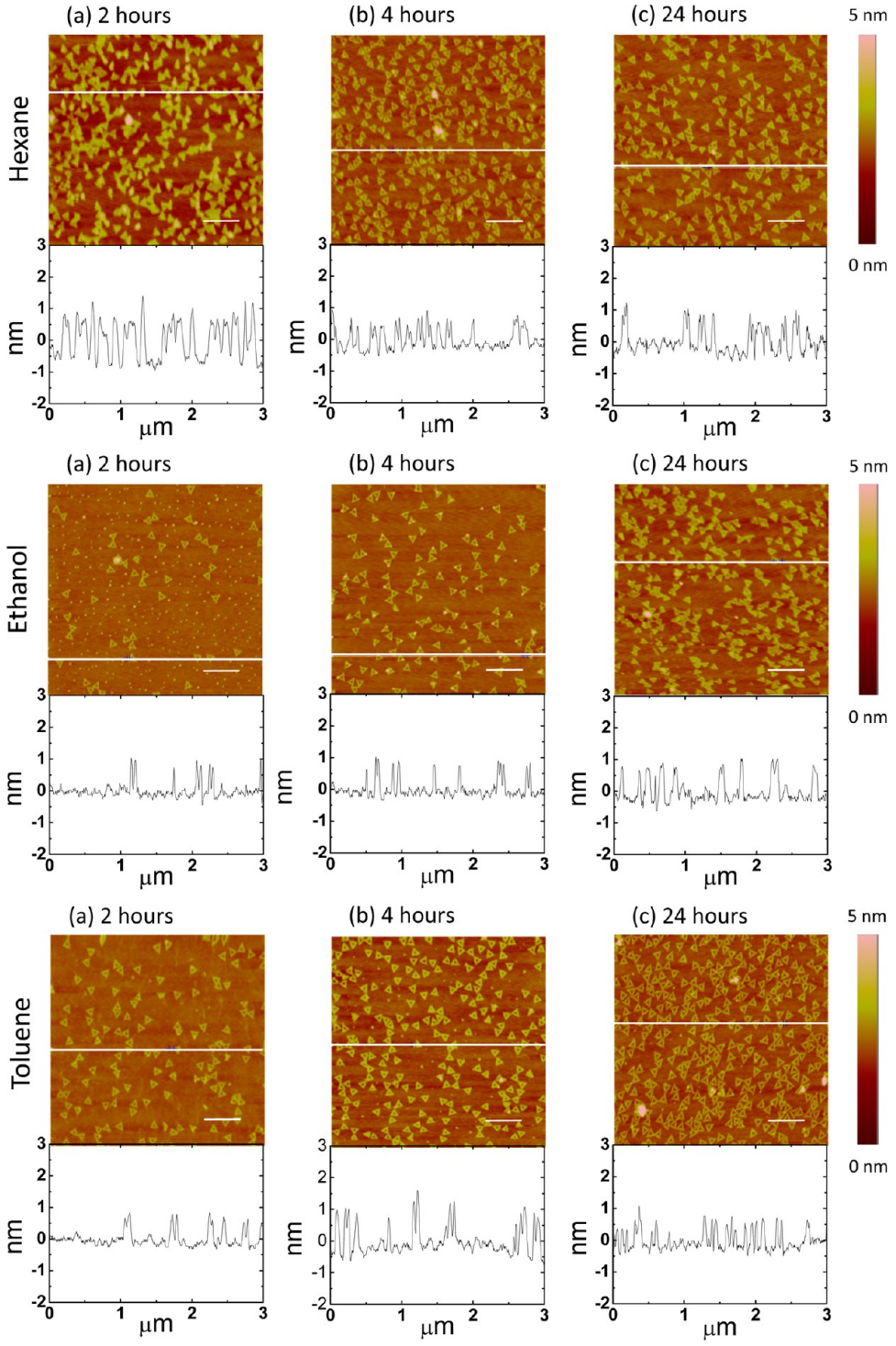

Figure 3. Stability of DNA nanostructures in organic solvents. AFM images of DNA origami triangles immersed in hexane (top), ethanol (middle), and toluene (bottom) for (a) 2 h, (b) 4 h, and (c) 24 h. White horizontal lines on the AFM images indicate the location of the cross sections. Scale bars: 500 nm.

under both argon and air and remained stabilized at higher temperature. However, the triangular features were preserved even after heating at 300 °C. We suspect that the remaining triangular feature at 250 and 300 °C is the inorganic residue (e.g., magnesium phosphate) after DNA decomposition. The atmosphere (air or argon) does not affect the average height of the structures at the entire range of heating temperature, suggesting that the decomposition of DNA is most likely thermal in nature and does not involve oxidation (Figure 2). Note that small decreases of the height were observed at <200 °C, which we attribute to the change in the hydration and/or physical deformation of the DNA. Overall, our result is consistent with the thermal stability of bulk DNA characterized by TGA.[43]

Effect of Rinsing with Organic Solvents and Aqueous Solutions. Solution chemistry plays a significant role in many bottom-up fabrication processes. For example, solution phase deposition of metal on DNA nanostructure has been explored

dx.doi.org/10.1021/cm5019663 | *Chem. Mater.* 2014, 26, 5265−5273

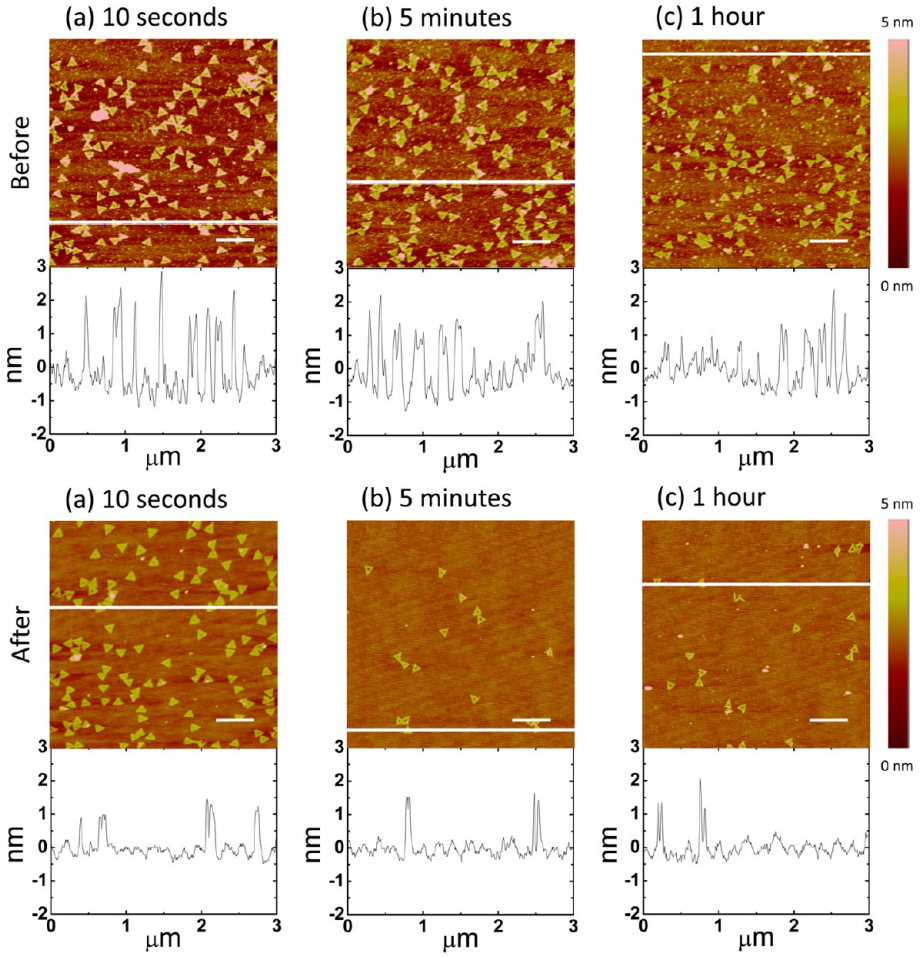

Figure 4. Stability of DNA nanostructures in deionized water. AFM images of DNA origami triangles before (top) and after (bottom) immersed in DI water for (a) 10 s, (b) 5 min, and (c) 1 h. White horizontal lines on the AFM images indicate the location of the cross sections. Scale bars: (a–c) 500 nm.

by several groups to fabricate metal and graphene nanostructures.[13−18,27] A major concern of solution phase processing of deposited DNA nanostructure is the danger of lifting-off the DNA nanostructure from the substrate. To evaluate this possibility, we have investigated the stability of deposited DNA nanostructure after immersion in organic solvents and aqueous solutions. Hexane, ethanol, and toluene were chosen to test the stability of DNA nanostructures in polar and nonpolar organic solvents. Deionized water and NaCl solutions were selected to test the effects of ionic strength. Effects of pH on DNA nanostructures were observed with hydrochloric acid and sodium hydroxide solutions. The wafers with the DNA origami triangles were characterized with AFM before and after the immersion to assess change of structure and number density of the DNA nanostructures.

To assess the stability of DNA nanostructures in organic solvents, DNA origami triangles were deposited onto silicon wafers and the substrates were immersed in organic solvents for up to 24 h. DNA nanostructures were characterized with AFM to evaluate their number density and the overall shape. Figure 3 shows the AFM images of DNA origami triangles after immersion in hexane, ethanol, and toluene for 2, 4, and 24 h. We observed that the surface coverage of DNA nanostructures on the silica substrates remained high even after 24 h of the immersion in organic solvents while the overall shapes of DNA nanostructures were well maintained. The height of the DNA nanostructures varied between ∼1 nm and ∼2 nm. We attribute the observed variation of the height to the variations in sample-tip and substrate-tip interaction although we cannot completely rule out the possibility of small molecule (e.g., solvent, impurities) intercalating into the DNA nanostructures.

To test the stability in aqueous solutions, the silicon substrates with DNA origami triangles were immersed into deionized water for up to 1 h. Figure 4 shows the AFM images of DNA origami triangles before and after immersion in deionized water for 10 s, 5 min, and 1 h. We observed a significant decrease in the density of the DNA nanostructures for even 10 s of immersion. The shape of the remaining DNA nanostructure showed significant variation between experiments. For example, after 5 min of immersion, in one experiment (Figure 4b bottom), most of the remaining DNA nanostructures appeared to be intact while in another (Figure S1b bottom in the Supporting Information) significantly damaged the DNA origami triangles were observed. Currently, we do not know what the cause of the irreproducibility although we suspect that the amount of Mg^{2+} adsorbed on silica surface may play a role. It has been suggested that the adsorption of DNA onto the SiO_2 substrate is mediated by adsorbed Mg^{2+}.

To evaluate the effect of the ionic strength, the silicon substrates with DNA origami triangles were immersed into NaCl solutions at different concentrations. Figure 5 shows the

dx.doi.org/10.1021/cm5019663 | *Chem. Mater.* 2014, 26, 5265−5273

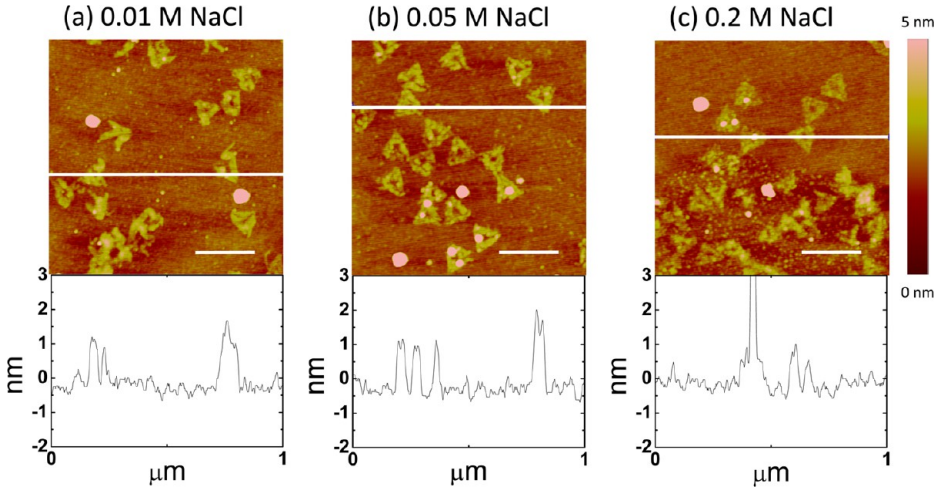

Figure 5. Effect of ionic strength on DNA nanostructures. AFM images of DNA origami triangles after immersed in (a) 0.01 M, (b) 0.05 M, and (c) 0.2 M NaCl solution for 10 s. White horizontal lines on the AFM images indicate the location of the cross sections. Scale bars: 250 nm.

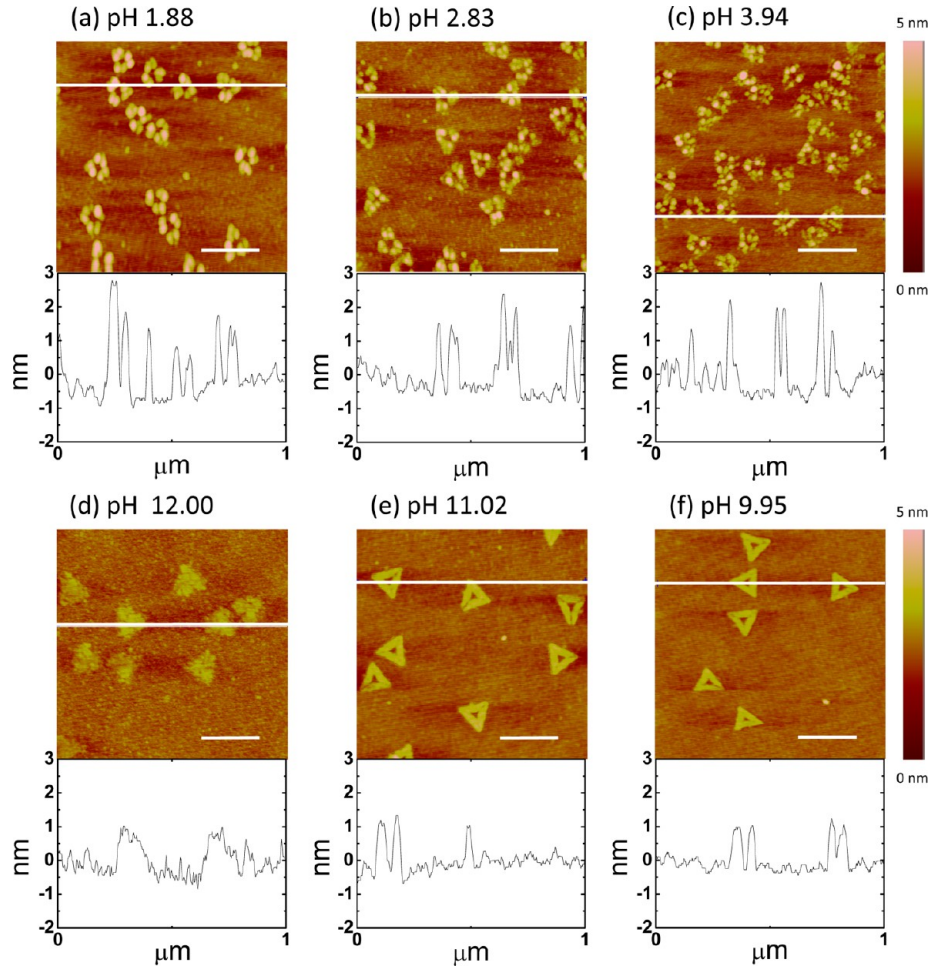

Figure 6. Effect of pH on DNA nanostructures. AFM images of DNA origami triangles immersed in (a) pH 1.88, (b) pH 2.83, (c) pH 3.94, (d) pH 12.00, (e) pH 11.02, and (f) pH 9.95 solutions for 10 s. White horizontal lines on the AFM images indicate the location of the cross sections. Scale bars: 250 nm.

AFM images of DNA nanostructures after immersion in 0.01, 0.05, and 0.2 M NaCl solutions for 10 s. Before AFM imaging, these samples were also washed several times with 9/1 (v/v) ethanol/water solution to remove the salt residues from the surface. We observed that the DNA nanostructures partially disintegrated after immersion into NaCl solutions, similar to the case with water immersion. In addition to the structural deformation, we also observed a decrease in the density of DNA nanostructure, indicating that the DNA nanostructures were lifted-off during the process. One remarkable difference

dx.doi.org/10.1021/cm5019663 | *Chem. Mater.* 2014, 26, 5265−5273

between DI water and NaCl solution is irregular height within a single DNA nanostructure. While the heights of three trapezoidal sides of the single DNA origami triangle immersed in DI water were even, those of the DNA origami triangle immersed in NaCl solution were irregular and rough. The surface of the DNA nanostructure appeared to be grinded. For one of the samples immersed in 0.2 M NaCl, the height of the DNA nanostructure increased to ~10 nm, suggesting accumulation of salt on the DNA surface while the majority of DNA nanostructures were missing (Figure S2c in the Supporting Information). We believe that Na^+ may have replaced the adsorbed Mg^{2+} on the substrate and may also accumulated on the DNA nanostructures, leading to the reduced density, shape deformation, and the irregular height of the DNA origami triangles.

It is well-known that double-stranded DNA is unstable under extreme pH, and over time it undergoes hydrolysis resulting in degradation/denaturing of DNA. Hydrolysis of DNA occurs in three different locations, phosphodiester backbone, DNA bases, and glycosidic bonds, which connect the nucleobases to sugar in the backbone of DNA.[44] From a study of the reversible T4 DNA ligase reaction at 25 °C and pH 7, the hydrolysis of a DNA phosphodiester bond was found to be an exothermic reaction ($\Delta G^{\circ\prime}$ = −5.3 kcal/mol).[45] This reaction, however, occurs extremely slow in biological conditions. Working with model compounds, the half-life of the hydrolysis through the C−O bond cleavage and the P−O bond cleavage at 25 °C were estimated to be 140 000 years and 30 000 000 years, respectively.[46,47] As the pH of the buffer solution increased, the rate constant of the hydrolysis at the C−O bond at 150 °C decreased by about 2 orders of the magnitude from pH 3 to 5 then stabilized afterward to pH 13, while it decreased by about three orders of the magnitude from pH 3 to 6.5 and then increased again about an order of the magnitude from pH 12 to 14 at the P−O bond at 250 °C. DNA bases can undergo hydrolytic deamination in which cytosine residue is converted to uracil residue. The rates of the cytosine deamination were determined with *Escherichia coli* DNA at 100 °C.[48] The rate decreased slowly in the pH range 6−8, reaching a minima at pH 8−8.5 and increased rapidly above pH 8.5. Hydrolysis of the glycosidic bonds in DNA mainly occurs at purines; the purine bases are released from DNA about 20 times faster than the pyrimidine bases are.[49] The pH dependence on the rate of the depurination was investigated with ^{14}C labeled *Bacillus subtilis* DNA in buffer at 70 °C.[50] In the pH 4.5−6.0 range, the reaction rate decreased by 1 order of magnitude for every increase of one pH unit. In the pH 6.0−7.5 range, the rate was less sensitive to pH and decreased about 1 order of magnitude per one and a half pH unit increment. These results indicate that the reaction of the depurination occurs by acid-catalyzed hydrolysis in acidic pH range. Therefore, a neutral pH, buffered environment is essential for DNA stability based on these studies.

The pH stability of the DNA nanostructures was evaluated by immersion in acidic and basic solutions (Figure 6 and Figures S3 and S4 in the Supporting Information). We observed that DNA origami triangles were highly unstable under acidic environment, and a mere 10 s immersion in a pH 4 solution resulted in its degradation. In contrast to the acidic environment, DNA origami triangles were stable up to pH 11 in a basic solution. Figure 6 shows the AFM images of DNA nanostructures after immersion in hydrochloric acid and sodium hydroxide solutions whose pH ranges are 2−4 and 10−12, respectively. Although there was no obvious decrease in the number density of DNA nanostructures after the immersion in both acidic and basic solutions, the distinct disintegration patterns were observed in both environments. Upon immersion into pH 2 solution, the DNA origami triangles disintegrated into six distinct pieces (Figure 6a). The trapezoidal sides of the DNA origami triangles fell apart and each side also broke in half (Figure 7b). By comparison between the disintegration pattern

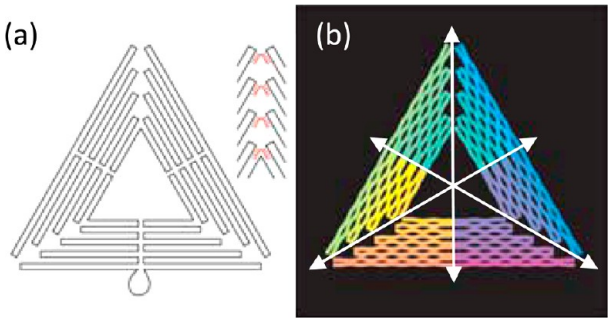

Figure 7. (a) Folding path of scaffold strand DNA in DNA origami triangle. Red lines are staple strands which bridge the trapezoidal sides. (b) Acidic hydrolysis disintegration pattern on bending path of helices at and away from crossovers. Adapted with permission from Macmillan Publishers Ltd. *Nature*, Rothemund, P. W. K. Folding DNA to Create Nanoscale Shapes and Patterns. *Nature* **2006**, *440*, 297−302. Copyright 2006 (ref 4).

and the folding path of the scaffold DNA strand (Figure 7a), it was clear that the disintegration initiated at tips and midpoints of the trapezoidal sides of the DNA origami triangle. At these locations, the scaffold DNA strand was bent four or five times and supported with a single scaffold and multiple staple strands. We hypothesize that these points are relatively weak compared to other parts within the DNA origami triangle due to the intensive folding and/or the lack of support of the scaffold strand. In contrast, a random disintegration pattern was observed at pH 4 (Figure 6c and Figure S3g−i in the Supporting Information). It is thought that the concentration of HCl becomes lower as pH becomes higher and the DNA nanostructures become unstable due to the low ionic strength, similar to the case of immersion in water. Under pH 12, the overall triangular shape was maintained; however, the details of the DNA nanostructure were blurred (Figure 6d and Figure S4a in the Supporting Information). It is likely that both dehybrization and hydrolysis could contribute to this observation; further study is needed to understand this behavior.

Degradation of DNA Origami Nanostructures with UV/O_3. We chose UV/O_3 oxidation as a model to evaluate the stability of DNA nanostructure under highly oxidative environments. UV/O_3 is a commonly used method to remove organic compound from surface. It is widely used to clean the surface and is an integral part of many atomic layer deposition procedures.[51−55]

In a typical experiment, a silicon wafer with deposited DNA origami triangles was exposed to UV/O_3 at room temperature for a fixed amount of time and then examined by AFM. Figure 8 shows the AFM images of DNA nanostructures before and after the UV/O_3 exposure. It was found that the DNA nanostructures survived 5 min exposure to UV/O_3 as indicated in Figure 9. The average height of the DNA nanostructure decreased by ~45% after exposure to UV/O_3 for 15 min and

dx.doi.org/10.1021/cm5019663 | *Chem. Mater.* 2014, 26, 5265−5273

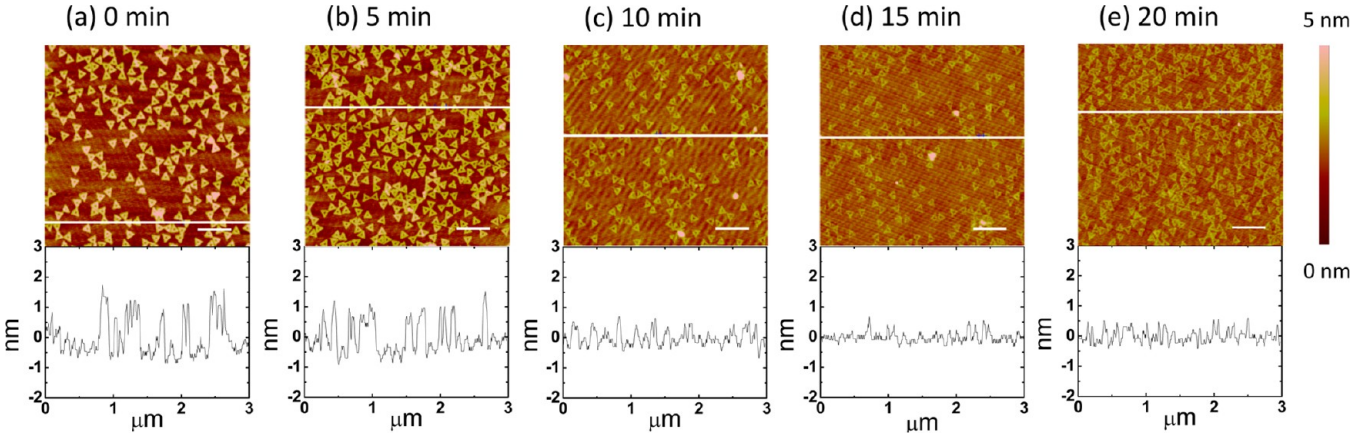

Figure 8. Effect of UV/O_3 on DNA nanostructures. AFM images of DNA origami triangles (a) before and after (b) 5 min, (c) 10 min, (d) 15 min, and (e) 20 min of the UV/O_3 treatments. White horizontal lines on the AFM images indicate the location of the cross sections. Scale bars: 500 nm.

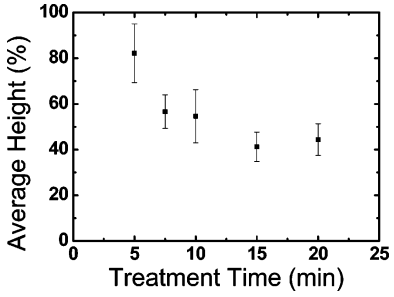

Figure 9. Change in average height of DNA nanostructures after the UV/O_3 exposure (n = 21–25). The data are normalized to the average height before the UV/O_3 exposure.

remained constant afterward. Interestingly, even after prolonged exposure, the overall triangular feature was consistently observed. This behavior is similar to the case of thermal annealing of DNA nanostructure. Similarly, we attribute these persisting triangular features to the inorganic residues of DNA decomposition.

CONCLUSION

In conclusion, our experimental studies on DNA nanostructures assembled on silicon substrates demonstrate the following: (1) The shape of the DNA nanostructures can be maintained at up to 200 °C under both Ar and air atmosphere. On heating beyond 200 °C, the DNA nanostructure decomposes. During the revision of this work, Pillers et al. reported the thermal stability of DNA origami nanostructures deposited on the mica surface.[56] Their work showed that DNA origami structures were still intact after 10 min heating at 150 °C while they degraded after heating at 250 °C; (2) DNA nanostructures are stable in common organic solvents for at least 24 h; (3) DNA nanostructure disintegrates under high and low ionic strength medium and lifts-off from the SiO_2 surface; (4) DNA nanostructures are stable in the pH range 7–11, and the pH above or below this range results in deformation of the overall structure; (5) upon exposure to UV/O_3, the DNA nanostructure survives 5 min and degrades uniformly in less than 15 min. Although chemically labile, our results clearly show that the topography of DNA nanostructure can indeed withstand very harsh chemical processing conditions and suggest that the application window of DNA nanostructure can be significantly wider than previously believed.

ASSOCIATED CONTENT

Supporting Information

Additional AFM images of DNA origami triangles. This material is available free of charge via the Internet at http://pubs.acs.org.

AUTHOR INFORMATION

Corresponding Author

*E-mail: hliu@pitt.edu.

Notes

The authors declare no competing financial interest.

ACKNOWLEDGMENTS

This work is supported by ONR (N000141310575) and AFOSR (FA9550-13-1-0083).

REFERENCES

(1) Andersen, E. S.; Dong, M.; Nielsen, M. M.; Jahn, K.; Lind-Thomsen, A.; Mamdouh, W.; Gothelf, K. V.; Besenbacher, F.; Kjems, J. *ACS Nano* **2008**, *2*, 1213.
(2) Han, D.; Pal, S.; Nangreave, J.; Deng, Z.; Liu, Y.; Yan, H. *Science* **2011**, *332*, 342.
(3) Ke, Y.; Ong, L. L.; Shih, W. M.; Yin, P. *Science* **2012**, *338*, 1177.
(4) Rothemund, P. W. K. *Nature* **2006**, *440*, 297.
(5) Wei, B.; Dai, M.; Yin, P. *Nature* **2012**, *485*, 623.
(6) Burns, J. R.; Stulz, E.; Howorka, S. *Nano Lett.* **2013**, *13*, 2351.
(7) Borman, S. *Chem. Eng. News* **2005**, *83*, 11.
(8) Gu, Q.; Cheng, C.; Gonela, R.; Suryanarayanan, S.; Anabathula, S.; Dai, K.; Haynie, D. T. *Nanotechnology* **2006**, *17*, R14.
(9) He, Y.; Chen, Y.; Liu, H.; Ribbe, A. E.; Mao, C. *J. Am. Chem. Soc.* **2005**, *127*, 12202.
(10) Paukstelis, P. J. *J. Am. Chem. Soc.* **2006**, *128*, 6794.
(11) Becerril, H. A.; Ludtke, P.; Willardson, B. M.; Woolley, A. T. *Langmuir* **2006**, *22*, 10140.
(12) Li, H.; Park, S. H.; Reif, J. H.; LaBean, T. H.; Yan, H. *J. Am. Chem. Soc.* **2003**, *126*, 418.
(13) Geng, Y.; Liu, J.; Pound, E.; Gyawali, S.; Harb, J. N.; Woolley, A. T. *J. Mater. Chem.* **2011**, *21*, 12126.
(14) Nakao, H.; Shiigi, H.; Yamamoto, Y.; Tokonami, S.; Nagaoka, T.; Sugiyama, S.; Ohtani, T. *Nano Lett.* **2003**, *3*, 1391.
(15) Pilo-Pais, M.; Goldberg, S.; Samano, E.; LaBean, T. H.; Finkelstein, G. *Nano Lett.* **2011**, *11*, 3489.
(16) Zheng, J.; Constantinou, P. E.; Micheel, C.; Alivisatos, A. P.; Kiehl, R. A.; Seeman, N. C. *Nano Lett.* **2006**, *6*, 1502.
(17) Liu, J.; Geng, Y.; Pound, E.; Gyawali, S.; Ashton, J. R.; Hickey, J.; Woolley, A. T.; Harb, J. N. *ACS Nano* **2011**, *5*, 2240.

(18) Pearson, A. C.; Liu, J.; Pound, E.; Uprety, B.; Woolley, A. T.; Davis, R. C.; Harb, J. N. *J. Phys. Chem. B* **2012**, *116*, 10551.
(19) Uprety, B.; Gates, E. P.; Geng, Y.; Woolley, A. T.; Harb, J. N. *Langmuir* **2014**, *30*, 1134.
(20) Malo, J.; Mitchell, J. C.; Vénien-Bryan, C.; Harris, J. R.; Wille, H.; Sherratt, D. J.; Turberfield, A. J. *Angew. Chem., Int. Ed.* **2005**, *44*, 3057.
(21) Shimada, J.; Maruyama, T.; Kitaoka, M.; Yoshinaga, H.; Nakano, K.; Kamiya, N.; Goto, M. *Chem. Commun.* **2012**, *48*, 6226.
(22) Keren, K.; Berman, R. S.; Buchstab, E.; Sivan, U.; Braun, E. *Science* **2003**, *302*, 1380.
(23) Li, S.; He, P.; Dong, J.; Guo, Z.; Dai, L. *J. Am. Chem. Soc.* **2004**, *127*, 14.
(24) Liu, Y. *Nat. Nanotechnol.* **2011**, *6*, 463.
(25) Becerril, H. A.; Woolley, A. T. *Small* **2007**, *3*, 1534.
(26) Deng, Z.; Mao, C. *Angew. Chem., Int. Ed.* **2004**, *43*, 4068.
(27) Jin, Z.; Sun, W.; Ke, Y.; Shih, C.-J.; Paulus, G. L. C.; Hua Wang, Q.; Mu, B.; Yin, P.; Strano, M. S. *Nat. Commun.* **2013**, *4*, 1663.
(28) Surwade, S. P.; Zhao, S.; Liu, H. *J. Am. Chem. Soc.* **2011**, *133*, 11868.
(29) Surwade, S. P.; Zhou, F.; Wei, B.; Sun, W.; Powell, A.; O'Donnell, C.; Yin, P.; Liu, H. *J. Am. Chem. Soc.* **2013**, *135*, 6778.
(30) Conway, J. W.; McLaughlin, C. K.; Castor, K. J.; Sleiman, H. *Chem. Commun.* **2013**, *49*, 1172.
(31) Keum, J.-W.; Bermudez, H. *Chem. Commun.* **2009**, 7036.
(32) Mei, Q.; Wei, X.; Su, F.; Liu, Y.; Youngbull, C.; Johnson, R.; Lindsay, S.; Yan, H.; Meldrum, D. *Nano Lett.* **2011**, *11*, 1477.
(33) Rajendran, A.; Endo, M.; Katsuda, Y.; Hidaka, K.; Sugiyama, H. *J. Am. Chem. Soc.* **2011**, *133*, 14488.
(34) Tagawa, M.; Shohda, K.-i.; Fujimoto, K.; Suyama, A. *Soft Matter* **2011**, *7*, 10931.
(35) Kornberg, A.; Baker, A. B. *DNA Replication*, 2nd ed.; University Science Books: Sausalito, CA, 2005; p 10.
(36) Vesenka, J.; Vellandi, C.; Kumar, I.; Marsh, T.; Henderson, E. *Scanning Microsc.* **1998**, *12*, 329.
(37) Albrechts, B.; Hautzinger, D. S.; Kruger, M.; Elwenspoek, M.; Muller, K.; Korvink, J. G. *Proceedings of the 21st Micromechanics and Micro Systems Europe Workshop*, Enschede, The Netherlands, September 26−29, 2010.
(38) Kershner, R. J.; Bozano, L. D.; Micheel, C. M.; Hung, A. M.; Fornof, A. R.; Cha, J. N.; Rettner, C. T.; Bersani, M.; Frommer, J.; Rothemund, P. W. K.; Wallraff, G. M. *Nat. Nanotechnol.* **2009**, *4*, 557.
(39) Carta, G.; El Habra, N.; Crociani, L.; Rossetto, G.; Zanella, P.; Zanella, A.; Paolucci, G.; Barreca, D.; Tondello, E. *Chem. Vap. Deposition* **2007**, *13*, 185.
(40) Lim, B. S.; Rahtu, A.; Gordon, R. G. *Nat. Mater.* **2003**, *2*, 749.
(41) Niinisto, J.; Putkonen, M.; Niinisto, L.; Stoll, S. L.; Kukli, K.; Sajavaara, T.; Ritala, M.; Leskela, M. *J. Mater. Chem.* **2005**, *15*, 2271.
(42) Khandelwal, G.; Bhyravabhotla, J. *PLoS One* **2010**, *5*, e12433.
(43) Aoi, K.; Takasu, A.; Okada, M. *Polymer* **2000**, *41*, 2847.
(44) Gates, K. S. *Chem. Res. Toxicol.* **2009**, *22*, 1747.
(45) Dickson, K. S.; Burns, C. M.; Richardson, J. P. *J. Biol. Chem.* **2000**, *275*, 15828.
(46) Schroeder, G. K.; Lad, C.; Wyman, P.; Williams, N. H.; Wolfenden, R. *Proc. Natl. Acad. Sci. U.S.A.* **2006**, *103*, 4052.
(47) Wolfenden, R.; Ridgway, C.; Young, G. *J. Am. Chem. Soc.* **1998**, *120*, 833.
(48) Lindahl, T.; Nyberg, B. *Biochemistry* **1974**, *13*, 3405.
(49) Lindahl, T. *Nature* **1993**, *362*, 709.
(50) Lindahl, T.; Nyberg, B. *Biochemistry* **1972**, *11*, 3610.
(51) Chang, C.-Y.; Lan, T.-W.; Chi, G.-C.; Chen, L.-C.; Chen, K.-H.; Chen, J.-J.; Jang, S.; Ren, F.; Pearton, S. J. *Electrochem. Solid-State Lett.* **2006**, *9*, G155.
(52) Crespo-Quesada, M.; Andanson, J.-M.; Yarulin, A.; Lim, B.; Xia, Y.; Kiwi-Minsker, L. *Langmuir* **2011**, *27*, 7909.
(53) Delabie, A.; Swerts, J.; Elshocht, S. V.; Jung, S.-H.; Raisanen, P. I.; Givens, M. E.; Shero, E. J.; Peeters, J.; Machkaoutsan, V.; Maes, J. W. *J. Electrochem. Soc.* **2011**, *158*, D259.
(54) Hämäläinen, J.; Puukilainen, E.; Sajavaara, T.; Ritala, M.; Leskelä, M. *Thin Solid Films* **2013**, *531*, 243.
(55) Rampelberg, G.; Schaekers, M.; Martens, K.; Xie, Q.; Deduytsche, D.; De Schutter, B.; Blasco, N.; Kittl, J.; Detavernier, C. *Appl. Phys. Lett.* **2011**, *98*, 162902.
(56) Pillers, M. A.; Lieberman, M. *J. Vac. Sci. Technol., B* **2014**, *32*, 040602.